Eur. Phys. J. D **7**, 235–242 (1999)

THE EUROPEAN PHYSICAL JOURNAL D

EDP Sciences
© Società Italiana di Fisica
Springer-Verlag 1999

Properties of pulsed entangled two-photon fields

J. Peřina Jr.[a]

Joint Laboratory of Optics of Palacký University and Institute of Physics of the Academy of Sciences of the Czech Republic, 17. listopadu 50, 772 07 Olomouc, Czech Republic

Received: 23 December 1998 / Received in final form: 14 April 1999

Abstract. The dependence of one- and two-photon characteristics of pulsed entangled two-photon fields generated in spontaneous parametric down-conversion on the pump-pulse properties (shape of the pump-pulse spectrum and its internal structure) is examined. It is shown that entangled two-photon fields with defined properties can be generated. A general relation between the spectra of the down-converted fields is established. As a special case the interference of two partially overlapping pulsed two-photon fields is studied. The fourth-order interference pattern of entangled two-photon fields is investigated in the polarization analog of the Hong-Ou-Mandel interferometer.

PACS. 42.65.-k Nonlinear optics – 42.65.Ky Harmonic generation, frequency conversion

1 Introduction

Over the last decades, the process of spontaneous parametric down-conversion in nonlinear crystals pumped by cw lasers has been extensively studied [1–3]. Nonclassical properties of entangled two-photon light generated by this process have been used many times for successful tests of quantum mechanics [2].

Recently a great deal of attention has been devoted to the properties of spontaneous parametric down-conversion pumped by femtosecond pulses. The main reason is that femtosecond pump-pulse duration may provide time synchronization of several entangled two-photon fields [4,5] and create this way more than two mutually entangled photon fields. Such fields have already been successfully used when observing quantum teleportation [6] and generating GHZ states [7–9]. The basic theoretical model of down-conversion process pumped by an (ultrashort) pulse has been developed in [10,11]. It has been studied in detail for a Gaussian pump pulse. It has been shown that ultrashort pump-pulse duration leads in general to a loss of visibility as a consequence of "partial" distinguishability of photons introduced by the pump pulse [10, 11]. Spectral aspects of the process are studied in [12]. The coincidence-count interference pattern has already been measured in the case when the down-converted fields propagate through narrow frequency filters [11,13]. The effect of dispersion in the down-converted fields on the coincidence-count interference pattern has been studied in [14]. Fourth-order interference of two two-photon down-converted fields has been investigated in the setting where the Mach-Zehnder interferometer is placed into the path of one of the output fields coming from the Hong-Ou-Mandel interferometer [15]. Pulsed parametric frequency conversion can also provide pulsed squeezed light [16].

In the above-mentioned papers a Gaussian pump-pulse spectrum has been assumed. In the paper we study how the pump-field spectral characteristics (shape and internal structure of the spectrum) influence the properties of down-converted fields. This may find an application in the generation of entangled two-photon fields with defined properties. Both one-photon (spectrum and time-dependent mean photon number) and two-photon (coincidence-count rates) characteristics are investigated. Two-photon characteristics are considered in the polarization analog of the Hong-Ou-Mandel interferometer. Because the down-converted fields are strongly influenced by the internal structure of the pump spectrum, we consider the case in which the overall pump spectrum is composed of the spectra of two mutually coherent ultrashort pulses. As a special case two-photon interference of two partially overlapping two-photon fields is investigated.

2 Spontaneous parametric down-conversion

The process of spontaneous parametric down-conversion is described by the following interaction Hamiltonian [1]:

$$\hat{H}_{\rm int}(t) = \int_{-L}^{0} {\rm d}z\, \chi^{(2)} E_p^{(+)}(z,t) \hat{E}_1^{(-)}(z,t) \hat{E}_2^{(-)}(z,t) + {\rm h.c.}, \tag{1}$$

where $\chi^{(2)}$ is the second-order susceptibility, $E_p^{(+)}$ denotes the positive-frequency part of the electric-field amplitude of the pump field, and $\hat{E}_1^{(-)}$ ($\hat{E}_2^{(-)}$) is the negative-frequency part of the electric-field operator of down-converted field 1 (2). The nonlinear crystal extends from

[a] e-mail: perina_j@sloup.upol.cz

$z=-L$ to $z=0$. The symbol h.c. means Hermitian conjugate.

The wave function $|\psi^{(2)}(0,t)\rangle$ describing an entangled two-photon state at $z=0$ (at the output plane of the crystal) for times t sufficiently long so that the nonlinear interaction is complete can be obtained in the form (for details, see [14])

$$|\psi^{(2)}(0,t)\rangle = C_\psi \exp[i(\omega_1^0+\omega_2^0)t]\int_{-L}^{0}\mathrm{d}z\int_{-\infty}^{\infty}\mathrm{d}\nu_p \times\int_{-\infty}^{\infty}\mathrm{d}\nu_1\int_{-\infty}^{\infty}\mathrm{d}\nu_2\,\mathcal{E}_p^{(+)}(0,\nu_p)\hat{a}_1^\dagger(\nu_1)\hat{a}_2^\dagger(\nu_2) \times\exp\left[i\left(\frac{\nu_p}{v_p}-\frac{\nu_1}{v_1}-\frac{\nu_2}{v_2}\right)z\right]\delta(\nu_p-\nu_1-\nu_2) \times\exp\left[i(\nu_1+\nu_2)t\right]|\mathrm{vac}\rangle, \quad (2)$$

where $\nu_j=\omega_j-\omega_j^0$ for $j=p,1,2$. The symbol $\mathcal{E}_p^{(+)}(0,\nu_p)$ denotes the spectrum of the positive-frequency part of the envelope of the pump-field amplitude at the output plane of the crystal; $\hat{a}_1^\dagger(\nu_1)$ $[\hat{a}_2^\dagger(\nu_2)]$ means the creation operator of the mode with wave vector k_1 (k_2) and frequency $\omega_1^0+\nu_1$ $(\omega_2^0+\nu_2)$ in down-converted field 1 (2). The symbol ω_j^0 stands for the central frequency of field j $(j=1,2,p)$ and $1/v_j$ denotes the inverse of group velocity of field j $[1/v_j=\mathrm{d}k_j/(\mathrm{d}\omega_{k_j})|_{\omega_{k_j}=\omega_j^0}]$. The susceptibility $\chi^{(2)}$ is included in the constant C_ψ. Frequency- and wave-vector phase matching for central frequencies $(\omega_p^0=\omega_1^0+\omega_2^0)$ and central wave vectors $(k_p^0=k_1^0+k_2^0)$, respectively, are assumed to be fulfilled when deriving equation (2). We note that the spontaneous parametric process is so weak that the pump-pulse depletion can be omitted even when intense ultrashort pump pulses are considered.

3 One-photon characteristics

The mean number of photons $\mathcal{N}_j$ in the down-converted field j is defined as

$$\mathcal{N}_j(\tau)=\langle\psi^{(2)}(0,t_0)|\hat{E}_j^{(-)}(0,t_0+\tau) \times\hat{E}_j^{(+)}(0,t_0+\tau)|\psi^{(2)}(0,t_0)\rangle, \quad (3)$$

where

$$\hat{E}_j^{(+)}(z_j,t_j)=\sum_{\nu_j}e_j(\nu_j)\hat{a}_j(\nu_j) \times\exp[ik_j^v(\omega_j^0+\nu_j)z_j-i(\omega_j^0+\nu_j)t_j]. \quad (4)$$

The symbol $e_j(\nu_j)$ denotes the amplitude per photon of the mode with the frequency $\omega_j^0+\nu_j$; k_j^v means a wave vector in vacuum in the j-th field. Substituting equations (2) and (4) into equation (3) we arrive at the expression for $\mathcal{N}_j$ in the form

$$\mathcal{N}_j(\tau)=\frac{(2\pi)^2|C_{\mathcal{N}_j}|^2}{|D|}\int_{-L}^{0}\mathrm{d}z\left|\mathcal{E}_p^{(+)}(0,\tau-D_{pj}z)\right|^2, \quad (5)$$

in which

$$D_{pj}=\frac{1}{v_p}-\frac{1}{v_j}=\Lambda+(-1)^j\frac{D}{2},\qquad j=1,2,$$
$$\Lambda=\frac{1}{v_p}-\frac{1}{2}\left(\frac{1}{v_1}+\frac{1}{v_2}\right),$$
$$D=\frac{1}{v_1}-\frac{1}{v_2}. \quad (6)$$

The symbol $\mathcal{E}_p^{(+)}(0,t)$ denotes the positive-frequency part of the envelope of the pump-field amplitude at the output plane of the crystal; $C_{\mathcal{N}_j}$ is a constant $[C_{\mathcal{N}_j}=\sqrt{2\pi}C_\psi\cdot e_j(\nu_j=0)]$. Because photons are in the nonlinear process generated in pairs, it holds that $\int_{-\infty}^{\infty}\mathrm{d}\tau\mathcal{N}_1(\tau)=\int_{-\infty}^{\infty}\mathrm{d}\tau\mathcal{N}_2(\tau)$.

If we consider the case in which $D_{pj}L\ll\tau_{\mathrm{char}}$, where τ_{char} is a characteristic time of the change of pump-field intensity, then, according to equation (5), the time dependence of $\mathcal{N}_j(\tau)$ resembles that of the pump field. This means that one-photon multimode Fock-state fields with a given mean-photon-number time dependence can be generated if the pump-field intensity is suitably chosen (see Fig. 2 in Sect. 5.1).

The spectrum $\mathcal{S}_j$ of the down-converted field j defined as

$$\mathcal{S}_j(\nu_j)=\langle\psi^{(2)}(0,t_0)|e_j^*(\nu_j)\hat{a}_j^\dagger(\nu_j)e_j(\nu_j)\hat{a}_j(\nu_j)|\psi^{(2)}(0,t_0)\rangle \quad (7)$$

can be obtained in terms of the pump-pulse spectrum:

$$\mathcal{S}_j(\nu_j)=|C_{\mathcal{S}_j}(\nu_j)|^2\int_{-\infty}^{\infty}\mathrm{d}\nu_p\left|\mathcal{E}_p^{(+)}(0,\nu_p)\right|^2 \times L^2\mathrm{sinc}^2\left[\frac{L}{2}\left(D_{p\,3-j}\nu_p-D\nu_j\right)\right], \quad (8)$$

where

$$\mathcal{E}_p^{(+)}(0,\nu_p)=\frac{1}{2\pi}\int_{-\infty}^{\infty}\mathrm{d}t\,\mathcal{E}_p^{(+)}(0,t)\exp(i\nu_p t), \quad (9)$$

$\mathrm{sinc}(x)=\sin(x)/x$, and $C_{\mathcal{S}_j}(\nu_j)=C_\psi e_j(\nu_j)$. According to equation (8), the spectrum of a down-converted field is obtained as a convolution of the pump-pulse spectrum with a function (sinc^2) characterizing phase-matching of the interacting fields in the nonlinear crystal. Oscillations in the spectrum $\mathcal{S}_j(\nu_j)$ occur for longer crystals if the pump-field spectrum $|\mathcal{E}_p^{(+)}(0,\nu_p)|^2$ has a peaked structure (for an example, see Fig. 3 in Sect. 5.1). The higher the number of peaks in the pump-field spectrum is, the smaller the amplitude and period of the oscillations are. For shorter crystals the sinc^2 function in equation (8) is wide and smooths out the peak structure of the pump-pulse spectrum $|\mathcal{E}_p^{(+)}(0,\nu_p)|^2$. This results in a suppression of oscillations in the spectrum $\mathcal{S}_j(\nu_j)$.

Equation (8) can be inverted and the pump-field spectrum $\left|\mathcal{E}_p^{(+)}(0,\nu_p)\right|^2$ may be determined from the spectrum $\mathcal{S}_j$. This is useful for the generation of a down-converted

field (in multimode Fock state) with a required spectrum, because the inverse formula to that in equation (8) provides a suitable profile of the pump-field spectrum.

If $|D_{p1}| \geq |D_{p2}|$, the spectrum $\mathcal{S}_1$ can be expressed in terms of the spectrum $\mathcal{S}_2$ as follows ($|C_{\mathcal{S}_j}(\nu_j)|^2 \equiv c_{\mathcal{S}_j}$ is assumed to be frequency independent for $j = 1, 2$):

$$\mathcal{S}_1(\nu_1) = \frac{c_{\mathcal{S}_1}}{c_{\mathcal{S}_2}} \int_{-\infty}^{\infty} \mathrm{d}\nu_2 p_{|D|L,d}(\nu_1 - \nu_2) \mathcal{S}_2\left(-\frac{\nu_2}{d}\right), \quad (10)$$

where $d = D_{p2}/D_{p1}$ and

$$p_{x,y}(\nu) = \frac{1}{\pi y} \int_0^x \mathrm{d}t \, \frac{x - |t|}{x - y|t|} \cos(\nu t). \quad (11)$$

The relation in equation (10) between the spectra of the down-converted fields is rather general and holds for an arbitrary pump field. This relation is a consequence of entanglement of photons emerging during their generation. It shows how photons in modes of the down-converted fields are correlated. Because the function $p(\nu)$ has a peak around $\nu = 0$ and goes to zero for larger values of ν, the mode with a given ν_1 has the strongest correlation with the mode of frequency $\nu_2 = -\nu_1/d$ (see Eq. (10)). It is worth noting that for $d < 0$ the strongest correlation occurs between modes at the same sides of the spectra.

4 Two-photon characteristics

Two-photon properties of down-converted fields determine results in coincidence-count measurements. Such measurements are conveniently described in terms of a two-photon amplitude $\mathcal{A}_{12}$ defined as follows:

$$\mathcal{A}_{12}(\tau_1, \tau_2) = \langle \mathrm{vac} | \hat{E}_1^{(+)}(0, t_0 + \tau_1) \times \hat{E}_2^{(+)}(0, t_0 + \tau_2) | \psi^{(2)}(0, t_0) \rangle. \quad (12)$$

Using the state $|\psi^{(2)}(0, t_0)\rangle$ given in equation (2), we arrive at the expression ($\omega_1^0 = \omega_2^0$ is assumed)

$$\mathcal{A}_{12}(T_0, \tau) = C_{\mathcal{A}} \frac{1}{|D|} \exp(-2i\omega_1^0 T_0) \mathrm{rect}\left(\frac{\tau}{DL}\right) \times \mathcal{E}_p^{(+)}\left(0, \frac{\Lambda}{D}\tau + T_0\right); \quad (13)$$

$\tau = \tau_1 - \tau_2$ and $T_0 = (\tau_1 + \tau_2)/2$. The symbol rect means the rectangular function ($\mathrm{rect}(x) = 1$ for $0 < x < 1$, $\mathrm{rect}(x) = 0$ otherwise); $C_{\mathcal{A}} = 2\pi e_1(\nu_1 = 0) e_2(\nu_2 = 0) C_\psi$.

We further consider one of the typical interferometric configurations, the polarization analog of the Hong-Ou-Mandel interferometer (see Fig. 1). Assuming type-II parametric down-conversion, two mutually perpendicularly polarized photons occur at the output plane of the crystal. They propagate through a birefringent material of a variable length l and then hit a 50/50 % beamsplitter. The coincidence-count rate R_c is then given by the number of simultaneously detected photons at both detectors D_A and D_B in a given time interval. Analyzers rotated by 45 degrees with respect to ordinary and extraordinary polarization directions of the nonlinear crystal enable quantum interference between two paths leading to a coincidence count; either a photon from field 1 is detected by the detector D_A and a photon from field 2 by the detector D_B or *vice versa*. The normalized coincidence-count rate R_n in this setting can be expressed as follows [14]:

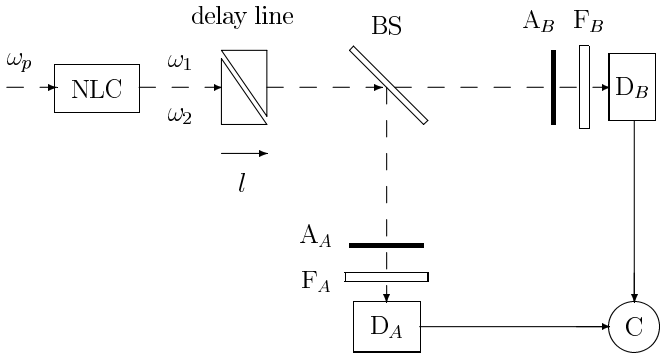

Fig. 1. Sketch of the system for coincidence-count measurement: pump pulse at the frequency ω_p generates in the nonlinear crystal NLC down-converted photons at the frequencies ω_1 and ω_2. They propagate through a delay line of the length l and are detected at the detectors D_A and D_B; BS denotes a beamsplitter, A_A and A_B are analyzers, F_A and F_B are frequency filters, and C means a coincidence device.

$$R_n(l) = 1 - \rho(l), \quad (14)$$

where

$$\rho(l) = \frac{1}{2R_0} \int_{-\infty}^{\infty} \mathrm{d}t_A \int_{-\infty}^{\infty} \mathrm{d}t_B \times \mathrm{Re}\left[\mathcal{A}_{12}\left(t_A - \frac{l}{g_1}, t_B - \frac{l}{g_2}\right) \times \mathcal{A}_{12}^*\left(t_B - \frac{l}{g_1}, t_A - \frac{l}{g_2}\right)\right] \quad (15)$$

and

$$R_0 = \frac{1}{2} \int_{-\infty}^{\infty} \mathrm{d}t_A \int_{-\infty}^{\infty} \mathrm{d}t_B \, |\mathcal{A}_{12}(t_A, t_B)|^2. \quad (16)$$

The symbol Re means real part; l is the length of a birefringent optical material (compare Fig. 1) with the group velocities g_1 and g_2 appropriate for the down-converted fields 1 and 2, respectively. Using the expression for $\mathcal{A}_{12}$ in equation (13), we get ($D > 0$ is assumed):

$$\rho(l) = \frac{|C_{\mathcal{A}}|^2}{2R_0 D^2} \int_{-DL/2+|\Delta\tau_l|}^{DL/2-|\Delta\tau_l|} \mathrm{d}\tau \int_{-\infty}^{\infty} \mathrm{d}T_0 \times \mathrm{Re}\left\{\mathcal{E}_p^{(+)}\left(0, \frac{\Lambda}{D}\tau + T_0\right) \mathcal{E}_p^{(-)}\left(0, -\frac{\Lambda}{D}\tau + T_0\right)\right\}, \quad (17)$$

$$R_0 = \frac{|C_{\mathcal{A}}|^2}{2D^2} \int_0^{DL} \mathrm{d}\tau \int_{-\infty}^{\infty} \mathrm{d}T_0 \left|\mathcal{E}_p^{(+)}\left(0, \frac{\Lambda}{D}\tau + T_0\right)\right|^2, \quad (18)$$

where $\Delta\tau_l = \tau_l - DL/2$ and

$$\tau_l = \left(\frac{1}{g_2} - \frac{1}{g_1}\right) l. \tag{19}$$

The analysis of the interference term $\rho(l)$ in equation (17) for an arbitrary pump field shows that $\rho(l)$ is nonzero only in the interval $0 \leq \tau_l \leq DL$. The interference pattern has the shape of a dip of the width DL. The change of envelope of the pump field leads only to a small modification of this shape. On the other hand, the internal structure of the pump field may result in the occurrence of peaks at the bottom of the dip (for an example, see Fig. 4 in Sect. 5.2). This behaviour follows if we consider the general relation between the shape of the two-photon amplitude and the profile of the interference pattern (for details, see [14]) for the two-photon amplitude $\mathcal{A}_{12}(T_0, \tau)$ given in equation (13).

Both one- and two-photon characteristics depend strongly on the internal structure of the pump-pulse spectrum. In experiment pump-pulse spectra with interesting internal structures can be obtained, *e.g.*, if we add spectra of several mutually coherent ultrashort pulses [17]. The pulses can be mutually delayed and have in general different widths and phase modulations of their spectra. We further pay attention to the case when the pump field is composed of two ultrashort pulses.

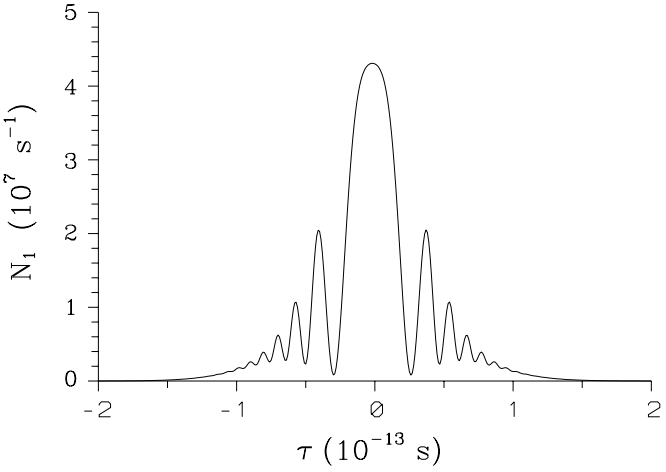

Fig. 2. Mean number of photons $N_1(\tau)$ of the signal field; $\tau_1 = 1\times10^{-13}$ s, $\tau_2 = 0.5\times10^{-13}$ s, $a_1 = 0$, $a_2 = 10$, $\xi_1 = \xi_2 = 1$, $L = 0.05$ mm, $\phi = 0$ rad, $\theta = 0$ s, $|C_{\mathcal{N}_1}|^2 = 1$ m^{-2}. In Figures 2–9, values of the inverse group velocities appropriate for the BBO crystal [18] with type-II interaction at the pump wavelength $\lambda_p = 413$ nm and at the down-conversion wavelengths $\lambda_1 = \lambda_2 = 826$ nm apply: $1/v_p = 56.85 \times 10^{-13}$ s/mm, $1/v_1 = 56.14 \times 10^{-13}$ s/mm, and $1/v_2 = 54.30 \times 10^{-13}$ s/mm. The optical material for the delay line is assumed to be quartz, for which $1/g_1 = 51.25 \times 10^{-13}$ s/mm and $1/g_2 = 51.59 \times 10^{-13}$ s/mm.

5 Effects of the internal structure of the pump-pulse spectrum

We assume that the pump field consists of two mutually delayed pulses with the amplitudes $\mathcal{E}_{p1}$ and $\mathcal{E}_{p2}$:

$$\mathcal{E}_p^{(+)}(0,t) = \mathcal{E}_{p1}^{(+)}(0,t) + \exp(i\phi)\mathcal{E}_{p2}^{(+)}(0,t+\vartheta), \tag{20}$$

where ϑ denotes a mutual delay between the pulses and ϕ stands for a relative phase of the pulses.

Pulses with Gaussian envelopes [17] are used in numerical calculations:

$$\mathcal{E}_{pj}^{(+)}(0,t) = \xi_j \exp\left(-\frac{1+ia_j}{\tau_j^2}t^2\right), \qquad j = 1,2. \tag{21}$$

The symbol ξ_j denotes the amplitude of the j-th pulse with duration τ_j and chirp parameter a_j. The spectrum $\mathcal{E}_{pj}^{(+)}(0,\nu_j)$ determined according to the definition in equation (9) is obtained in the form

$$\mathcal{E}_{pj}^{(+)}(0,\nu_j) = \xi_j \frac{\tau_j}{2\sqrt{\pi}\sqrt{1+ia_j}} \exp\left(-\frac{\tau_j^2}{4(1+ia_j)}\nu_j^2\right), \quad j = 1,2. \tag{22}$$

5.1 One-photon characteristics

For short crystals the time dependence of the mean number of photons $\mathcal{N}_j(t)$ in mode j resembles that of the pump field (see Sect. 3). So, *e.g.*, if the pump field consists of two femtosecond pulses of the same duration and one has no chirp whereas the other one is highly chirped, the overall pump field as well as $\mathcal{N}_j(t)$ have a peaked structure (see Fig. 2).

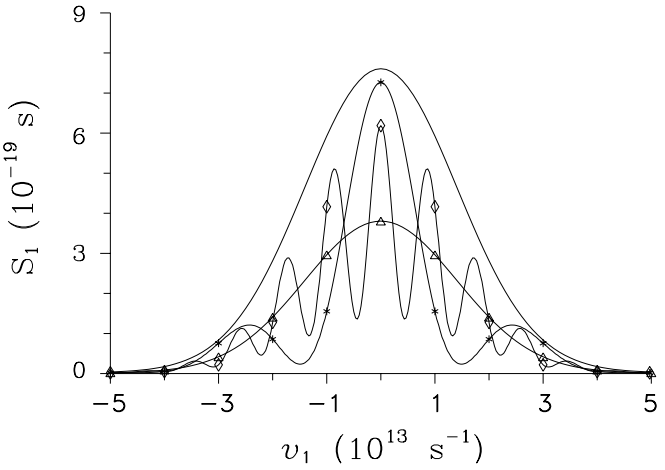

Fig. 3. Spectrum $S_1(\nu_1)$ of the signal field for various values of the delay ϑ; $\vartheta = 0$ s (solid curve without symbols), $\vartheta = 3 \times 10^{-13}$ s ($*$), $\vartheta = 10 \times 10^{-13}$ s ($\diamond$), and $\vartheta = 50 \times 10^{-13}$ s ($\triangle$); $\tau_1 = \tau_2 = 1 \times 10^{-13}$ s, $a_1 = a_2 = 0$, $\xi_1 = \xi_2 = 1$, $L = 10$ mm, $\phi = 0$ rad, and $|C_{\mathcal{S}_1}|^2 = 1$ m^{-2}.

Oscillations occur in the one-photon spectra S_1 and S_2, see Figure 3 for the signal spectrum S_1. The period as well as the amplitude of these oscillations decrease with increasing values of the delay ϑ as has been discussed in

section 3. A nonzero delay ϑ causes oscillations in the pump-field spectrum $|\mathcal{E}_p^{(+)}(0,\nu_p)|^2$ which are transferred through the phase-matching function (sinc^2 in equation (8)) into the spectra of the down-converted fields. These oscillations are well pronounced for longer crystals. If the pump pulses are in phase ($\phi = 0$ rad), there is maximum in the center of the spectrum. There occurs a local minimum in the center of the spectrum providing that the pump pulses are out of phase. Alternatively we may consider the overall down-converted field to be composed of two contributions from two down-conversion processes (pumped by two pump pulses) and then the origin of the oscillations lies in a coherent summation of these contributions in each frequency mode.

A suitable choice of the pump-field characteristics may provide down-converted fields with required one-photon properties. Down-converted fields with given properties can also be obtained by "passive methods", *e.g.*, by frequency filtering of fields already generated in the parametric process. However, entanglement of photons between two down-converted fields is partially disturbed in this case.

5.2 Two-photon characteristics

The formulas for the quantities ρ (17) and R_0 (18) can be recast into the following form if the pump field given in equation (20) is taken into account:

$$\rho(l,\vartheta,\phi) = \rho_1(l) + \rho_2(l,\vartheta,\phi), \tag{23}$$

$$\rho_1(l) = \frac{|C_{\mathcal{A}}|^2}{2R_0D^2}\int_{-DL/2+|\Delta\tau_l|}^{DL/2-|\Delta\tau_l|}\mathrm{d}\tau\int_{-\infty}^{\infty}\mathrm{d}T_0 \times \mathrm{Re}\left\{\sum_{j=1,2}\mathcal{E}_{pj}^{(+)}\left(0,\frac{\Lambda}{D}\tau+T_0\right)\times\mathcal{E}_{pj}^{(-)}\left(0,-\frac{\Lambda}{D}\tau+T_0\right)\right\}, \tag{24}$$

$$\rho_2(l,\vartheta,\phi) = \frac{|C_{\mathcal{A}}|^2}{R_0D^2}\int_{-DL/2+|\Delta\tau_l|}^{DL/2-|\Delta\tau_l|}\mathrm{d}\tau\int_{-\infty}^{\infty}\mathrm{d}T_0 \times \mathrm{Re}\left\{\exp(-i\phi)\mathcal{E}_{p1}^{(+)}\left(0,\frac{\Lambda}{D}\tau+T_0\right)\times\mathcal{E}_{p2}^{(-)}\left(0,-\frac{\Lambda}{D}\tau+T_0+\vartheta\right)\right\}, \tag{25}$$

$$R_0(\vartheta,\phi) = R_{01} + R_{02}(\vartheta,\phi), \tag{26}$$

$$R_{01} = \frac{|C_{\mathcal{A}}|^2L}{2|D|}\int_{-\infty}^{\infty}\mathrm{d}T_0\left[\sum_{j=1,2}\left|\mathcal{E}_{pj}^{(+)}(0,T_0)\right|^2\right], \tag{27}$$

$$R_{02}(\vartheta,\phi) = \frac{|C_{\mathcal{A}}|^2L}{|D|}\int_{-\infty}^{\infty}\mathrm{d}T_0\,\mathrm{Re}\left\{\exp(-i\phi)\mathcal{E}_{p1}^{(+)}(0,T_0)\times\mathcal{E}_{p2}^{(-)}(0,T_0+\vartheta)\right\}. \tag{28}$$

The expressions for ρ_1, ρ_2, R_{01}, and R_{02} for Gaussian pump pulses are contained in the Appendix.

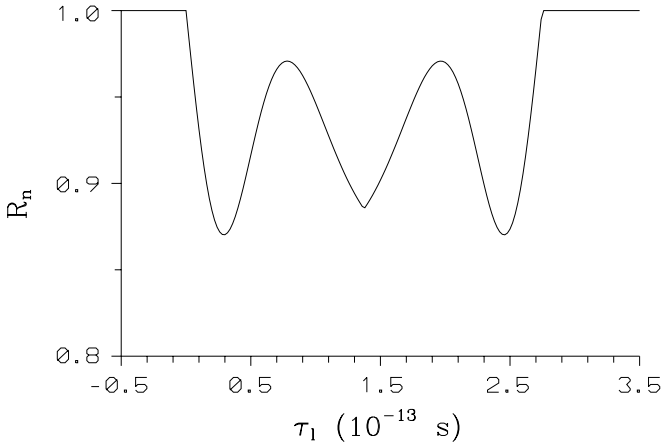

Fig. 4. The interference pattern in the normalized coincidence-count rate $R_n(\tau_l)$ shows three dips; $\tau_1 = 1\times10^{-13}$ s, $\tau_2 = 0.5\times10^{-13}$ s, $a_1 = a_2 = 0$, $\xi_1 = 1$, $\xi_2 = 1.5$, $L = 1.5$ mm, $\phi = \pi$ rad, and $|C_{\mathcal{A}}|^2 = 10$ m^{-2}.

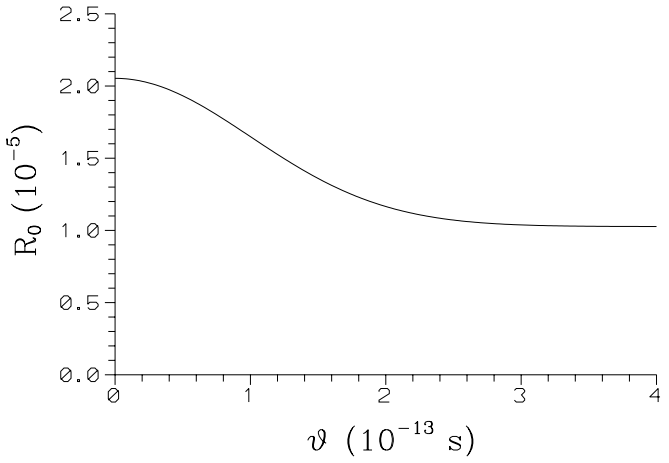

Fig. 5. Probability of a coincidence count R_0 as a function of the delay ϑ; $\tau_1 = \tau_2 = 1\times10^{-13}$ s, $a_1 = a_2 = 0$, $\xi_1 = \xi_2 = 1$, $L = 1.5$ mm, $\phi = 0$ rad, and $|C_{\mathcal{A}}|^2 = 10$ m^{-2}.

We demonstrate the general conclusions given in section 4 considering two Gaussian pump pulses of different time durations and being out of phase. The overall pump field then has positive values at the edges and is negative in the center and so the corresponding fourth-order interference pattern consists of three dips (see Fig. 4).

5.3 Interference of two entangled two-photon fields

A physically interesting case occurs if the overall pump field consists of two partially overlapping ultrashort pulses. Then the overall down-converted field can be considered as composed of two partially overlapping two-photon fields (see the expression for $\mathcal{A}_{12}$ in Eq. (13)). The two two-photon fields are mutually coherent and interfere. In the following we study the fourth-order interference of these fields in detail.

Fourth-order interference influences the coincidence-count probability. This probability is linearly proportional

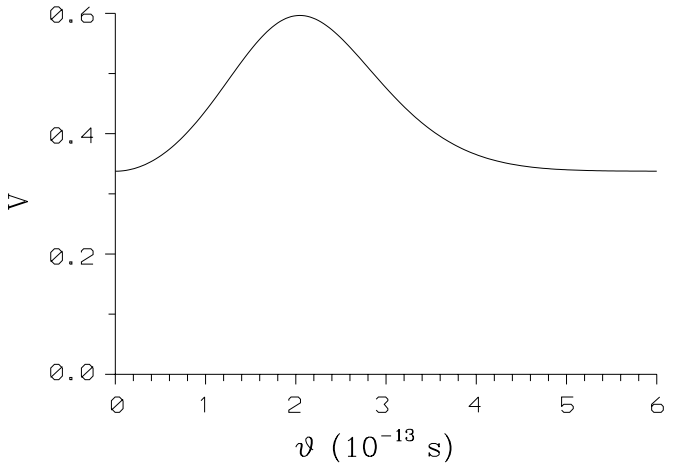

Fig. 6. Visibility V [$V = (R_{n,\max} - R_{n,\min})/(R_{n,\max} + R_{n,\min})$] as a function of the delay ϑ; values of the parameters are the same as in Figure 5.

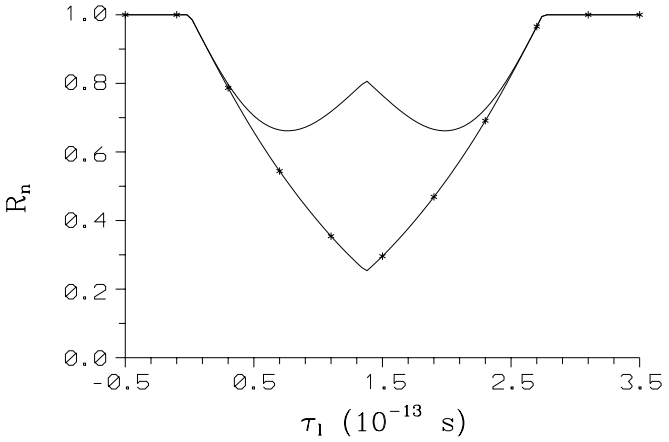

Fig. 7. Interference pattern in the normalized coincidence-count rate $R_n(\tau_l)$ for various phases ϕ: $\phi = \pi$ rad (solid curve without symbols) and $\phi = 0$ rad (solid curve with $*$); $\vartheta = 2.04 \times 10^{-13}$ s; values of the other parameters are the same as in Figure 5.

to the quantity $R_0(\vartheta, \phi)$ which is shown in Figure 5 as a function of the mutual delay ϑ of the pump pulses in the case when two pump pulses are in phase ($\phi = 0$ rad). The coincidence-count probability decreases with increasing ϑ and is twice for completely overlapping entangled two-photon fields ($\vartheta = 0$ s) than in the case where there is no overlap ($\vartheta \to \infty$ s). This dependence reflects constructive interference between two entangled two-photon fields having its origin in the mutual coherence of the pump pulses.

The fourth-order interference pattern in the polarization analog of the Hong-Ou-Mandel interferometer behaves as follows. The visibility V of the coincidence-count pattern (coincidence-count dip [1]) as a function of the delay ϑ is shown in Figure 6. For $\vartheta = 0$ s the entangled two-photon fields completely overlap, so, in fact, there is only one entangled two-photon field with a given visibility. As the delay ϑ increases, two entangled two-photon fields are gradually formed at the output plane of the crystal. When the delay ϑ increases, the overlap of the two entangled two-photon fields becomes smaller and higher values of the visibility V occur. This means that the distinguishability of the signal and idler photons decreases with increasing ϑ because the higher the visibility, the higher the distinguishability of the signal and idler photons [11]. For greater values of ϑ the visibility V decreases. When the pump pulses are delayed so much that they do not overlap there are two nonoverlapping down-converted fields and the visibility is back to the value appropriate for $\vartheta = 0$ s. The increase of the visibility V caused by partially overlapped entangled two-photon fields might be useful in various multiparticle experiments for which high visibilities are required. When the distinguishability of the signal and idler photons is minimum (V is maximum), we can already distinguish two entangled two-photon fields in the signal-field mean photon number $\mathcal{N}_1(t)$. We note that the value of the delay ϑ for which two entangled two-photon fields in a down-converted beam can be distinguished differs for the signal and idler fields as a consequence of different group velocities in the nonlinear crystal.

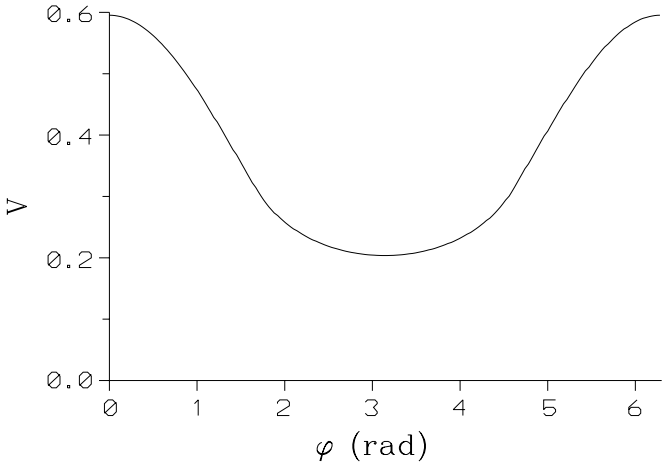

Fig. 8. Visibility V as a function of the relative phase ϕ; $\vartheta = 2.04 \times 10^{-13}$ s, values of the other parameters are the same as in Figure 5.

The relative phase ϕ influences the shape of coincidence-count pattern. There might occur a peak at the bottom of the dip if the pump pulses are not in phase ($\phi \neq 0$ rad, see Figure 7). This then results in a loss of visibility. The reason is that if the pump pulses are not in phase the overall two-photon amplitude $\mathcal{A}_{12}(T_0, \tau)$ gets phase modulation along T_0 (compare the expression for $\mathcal{A}_{12}$ in Eq. (13)) which then results in the loss of visibility (for a relation between the shapes of the two-photon amplitude $\mathcal{A}_{12}$ and the coincidence-count pattern described by R_n, see [14]). A typical dependence of the visibility V as a function of ϕ is depicted in Figure 8.

The value of the delay $\vartheta_{\max}$ for which there is a maximum visibility of the coincidence-count pattern increases with increasing pump pulse duration τ_0 (we assume $\tau_1 = \tau_2 = \tau_0$). This is demonstrated in Figure 9.

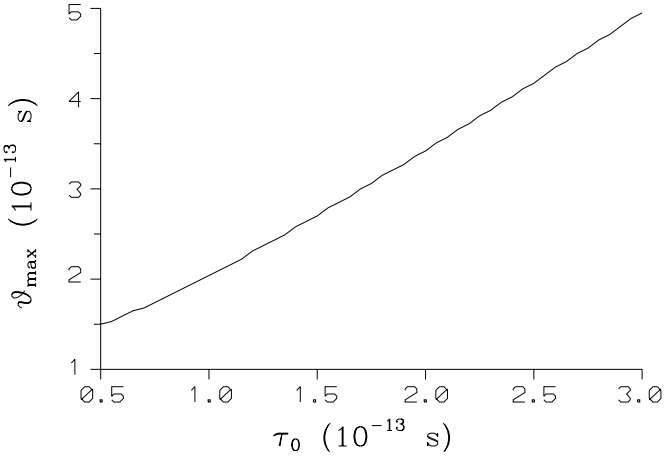

Fig. 9. Delay $\vartheta_{\max}$ corresponding to the maximum of the visibility $V(\vartheta)$ as a function of the pump pulse duration τ_0 ($\tau_0 = \tau_1 = \tau_2$); $a_1 = a_2 = 0$, $\xi_1 = \xi_2 = 1$, $L = 1.5$ mm, $\phi = 0$ rad, and $|C_{\mathcal{A}}|^2 = 10$ m^{-2}.

The value of $\vartheta_{\max}$ is influenced also by pump-pulse chirp. The higher the chirp, the lower the value of $\vartheta_{\max}$. However, nonzero chirp also results in the loss of visibility [14] because it leads to a phase modulation of the two-photon amplitude $\mathcal{A}_{12}$. Using this fact, the influence of chirp can be eliminated from the measured visibilities and the pump-pulse duration τ_0 may be in principle determined from the measured value of $\vartheta_{\max}$.

6 Conclusions

We have studied both one- and two-photon properties of entangled two-photon fields generated by spontaneous parametric down-conversion pumped by fields with arbitrary characteristics. The spectrum of a down-converted field may be expressed as a convolution of the pump-field spectrum with the function originating in phase-matching of waves in a nonlinear crystal. The spectra of the down-converted fields are mutually strongly correlated and a general relation between them independent of the pump-field parameters has been established. Both one- and two-photon properties depend strongly on the internal structure of the pump field. For example, there may occur oscillations in the spectrum of a down-converted field. One-photon multimode Fock-state fields with defined characteristics (intensity or spectrum profile) can be generated if the pump-field parameters are suitably chosen. For more complex pump fields a typical dip in the coincidence-count interference pattern of the polarization analog of the Hong-Ou-Mandel interferometer is replaced by more complex patterns which may be composed, *e.g.*, of two or three dips.

Properties of two (partially) overlapping entangled two-photon fields have also been investigated in detail. It has been shown that two entangled two-photon fields are mutually coherent if the corresponding pump pulses are coherent. Partial overlap of two entangled two-photon pulsed fields leads to higher values of the visibility of the coincidence-count interference pattern in comparison with those appropriate for one entangled two-photon field. This may be conveniently used in many multiparticle experiments for which high values of visibility are required.

The author thanks for a kind hospitality in Quantum Imaging Laboratory at Boston University. He also thanks J. Peřina for reading the manuscript. He acknowledges support from Grant No. VS96028 of the Czech Ministry of Education and Grant No. 19982003012 of the Czech Home Department.

Appendix: Coincidence-count interference pattern for two Gaussian pump pulses

The quantities ρ_1 in equation (24), ρ_2 in equation (25), R_{01} in equation (27), and R_{02} in equation (28) can be expressed in the following forms when Gaussian pump pulses are considered:

$$\rho_1(l) = \frac{\sqrt{\pi}|C_{\mathcal{A}}|^2}{2\sqrt{2}R_0D^2}\int_{-DL/2+|\Delta\tau_l|}^{DL/2-|\Delta\tau_l|}\mathrm{d}\tau \times\left\{\sum_{j=1,2}\xi_j^2\tau_j\exp\left[-2\left(\frac{|\alpha_j|\tau_j\Lambda\tau}{D}\right)^2\right]\right\}, \quad (A.1)$$

$$\rho_2(l,\vartheta,\phi) = \frac{\sqrt{\pi}|C_{\mathcal{A}}|^2\xi_1\xi_2}{R_0D^2}\int_{-DL/2+|\Delta\tau_l|}^{DL/2-|\Delta\tau_l|}\mathrm{d}\tau \times\mathrm{Re}\left\{\frac{\exp(-i\phi)}{\sqrt{\alpha_1+\alpha_2^*}}\exp\left[-\frac{\alpha_1\alpha_2^*}{\alpha_1+\alpha_2^*}\left(\vartheta-\frac{2\Lambda}{D}\tau\right)^2\right]\right\}, \quad (A.2)$$

$$R_{01} = \frac{\sqrt{\pi}|C_{\mathcal{A}}|^2L}{2\sqrt{2}|D|}\left[\xi_1^2\tau_1+\xi_2^2\tau_2\right], \quad (A.3)$$

$$R_{02}(\vartheta,\phi) = \frac{\sqrt{\pi}|C_{\mathcal{A}}|^2L\xi_1\xi_2}{|D|}\,\mathrm{Re}\left\{\frac{\exp(-i\phi)}{\sqrt{\alpha_1+\alpha_2^*}} \times\exp\left(-\frac{\alpha_1\alpha_2^*}{\alpha_1+\alpha_2^*}\vartheta^2\right)\right\}, \quad (A.4)$$

where $\alpha_j = (1+ia_j)/\tau_j^2$ for $j = 1, 2$.

References

1. L. Mandel, E. Wolf, *Optical Coherence and Quantum Optics* (Cambridge University Press, Cambridge, 1995), and references therein.
2. J. Peřina, Z. Hradil, B. Jurčo, *Quantum Optics and Fundamentals of Physics* (Kluwer, Dordrecht, 1994), and references therein.
3. J. Peřina, *Quantum Statistics of Linear and Nonlinear Optical Phenomena* (Kluwer, Dordrecht, 1991).
4. M. Zukowski, A. Zeilinger, M.A. Horne, A.K. Ekert, Phys. Rev. Lett. **71**, 4287 (1993).

5. J.-W. Pan, A. Zeilinger, Phys. Rev. A **57**, 2208 (1998).
6. D. Bouwmeester, J.-W. Pan, K. Mattle, M. Eibl, H. Weinfurter, A. Zeilinger, Nature **390**, 575 (1997).
7. D.M. Greenberger, M.A. Horne, A. Shimony, A. Zeilinger, Am. J. Phys. **58**, 1131 (1990).
8. D. Bouwmeester, J.-W. Pan, M. Daniell, H. Weinfurter, A. Zeilinger, Phys. Rev. Lett. **82**, 1345 (1999).
9. J.G. Rarity, P.R. Tapster, Phys. Rev. A **59**, R35 (1999).
10. T.E. Keller, M.H. Rubin, Phys. Rev. A **56**, 1534 (1997).
11. G. Di Giuseppe, L. Haiberger, F. De Martini, A.V. Sergienko, Phys. Rev. A **56**, R21 (1997).
12. W.P. Grice, I.A. Walmsley, Phys. Rev. A **56**, 1627 (1997).
13. W.P. Grice, R. Erdmann, I.A. Walmsley, D. Branning, Phys. Rev. A **57**, R2287 (1998).
14. J. Peřina, Jr., A.V. Sergienko, B.M. Jost, B.E.A. Saleh, M.C. Teich, Phys. Rev. A **59**, 2359 (1999).
15. T.E. Keller, M.H. Rubin, Y. Shih, Phys. Lett. A **244**, 507 (1998).
16. A. Beržanskis, K.-H. Feller, A. Stabinis, Opt. Commun. **155**, 155 (1998).
17. J.-C. Diels, W. Rudolph, *Ultrashort Laser Pulse Phenomena* (Academic Press, San Diego, 1996).
18. V.G. Dmitriev, G.G. Gurzadyan, D.N. Nikogosyan, *Handbook of Nonlinear Optical Crystals* (Springer, Berlin, 1997).